

Theoretical insights on hydrogen activation and diffusion behaviour on ZnO (10 $\bar{1}$ 0) surface

Zezhong Miao,^{ab} Xing Zhu,^c Yuqian Jin,^d Lingzhao Kong,^{*c} and Shenggang Li ^{*ab}

^aLow-Carbon Conversion Science and Engineering Centre, and State Key Laboratory of Low Carbon Catalysis and Carbon Dioxide Utilization, Shanghai Advanced Research Institute, Chinese Academy of Sciences, Shanghai 201210, China. E-mail: lisg@sari.ac.cn.

^bSchool of Physical Science and Technology, ShanghaiTech University, Shanghai 201210, China.

^cSchool of Environmental Science and Engineering, Suzhou University of Science and Technology, Suzhou, Jiangsu, 215009, China. E-mail: lizhkong@usts.edu.cn.

^dDepartment of Chemistry, University of California, Irvine, Irvine, CA 92697, USA.

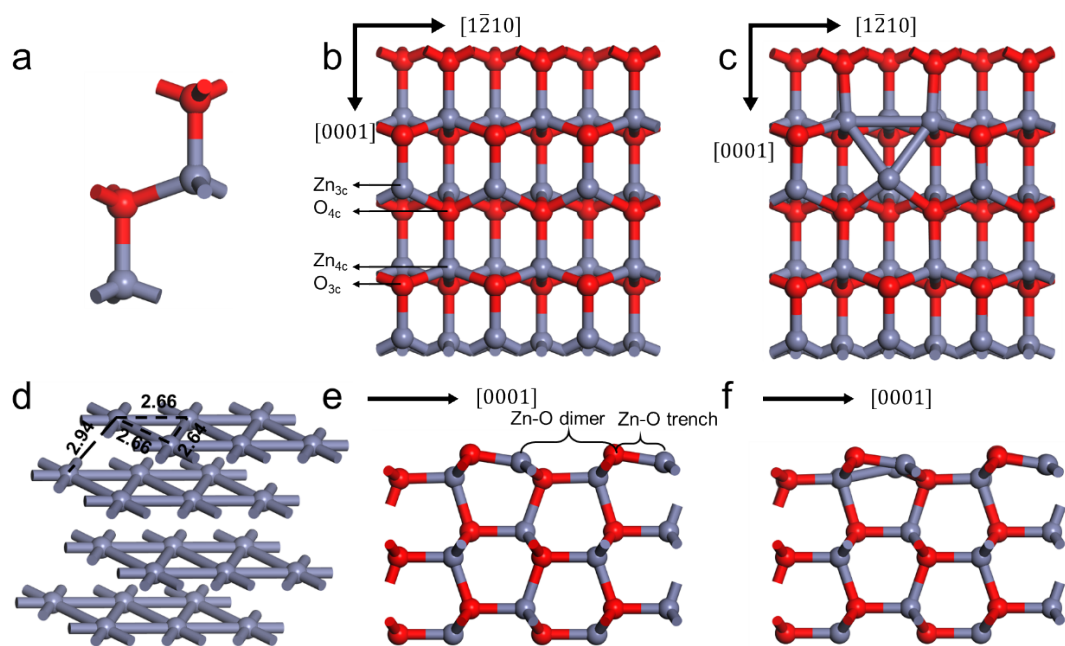


Figure S1. Schematic illustrations of several initial structures. (a) Primitive unit cell (PUC) of bulk ZnO; (b) top view and (e) side view of pristine ZnO $(10\bar{1}0)$ facet; (c) top view and (f) side view of defect ZnO $(10\bar{1}0)$ facet; (d) Pure metallic Zn. Gray balls represent Zn atoms, red balls denote O atoms.

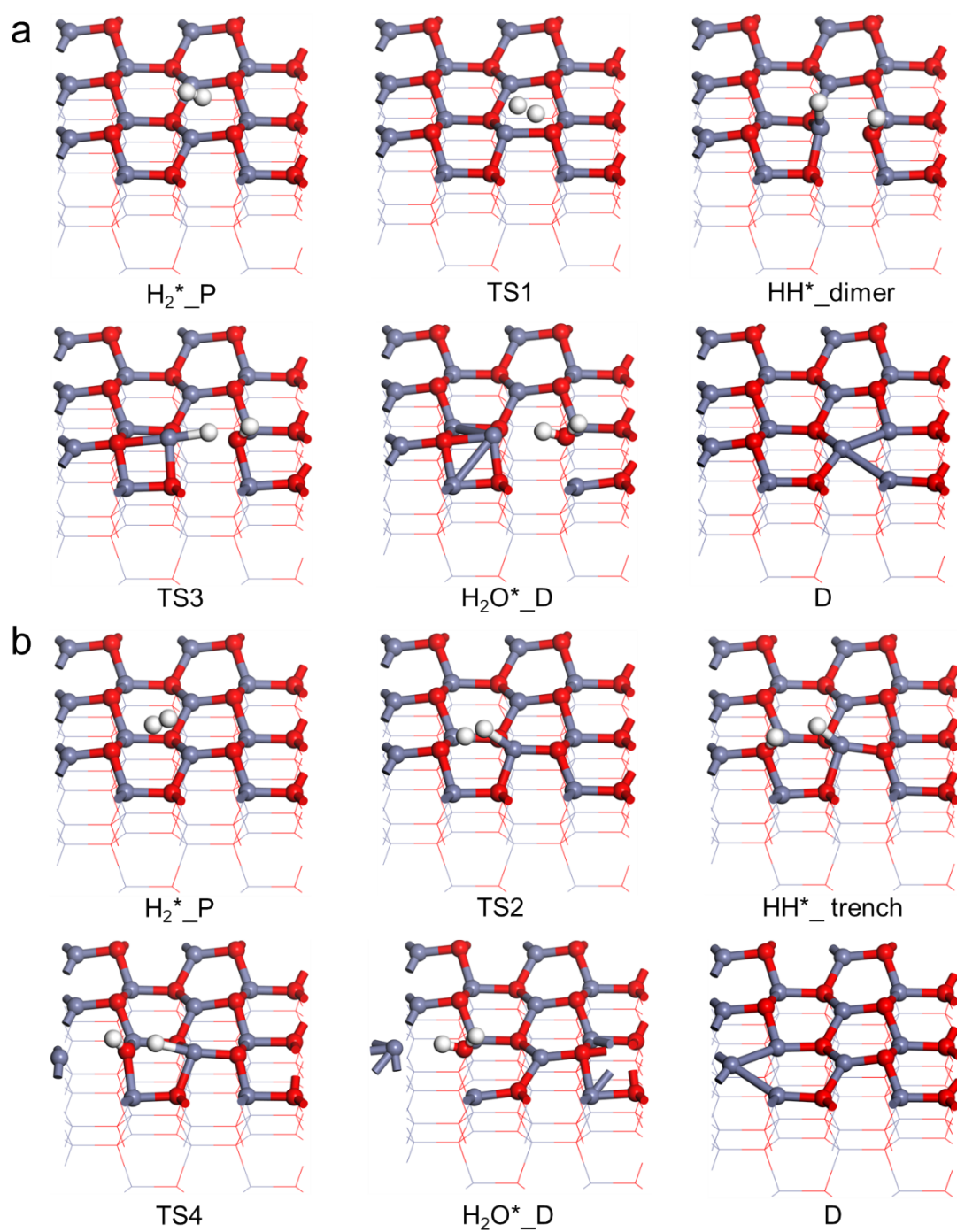


Figure S2. Representations of the key intermediates and transition states along (a) dimer-H and (b) trench-H induced oxygen-vacancies formation pathway. Gray balls represent Zn atoms, red balls denote O atoms and white spheres correspond to H atoms.

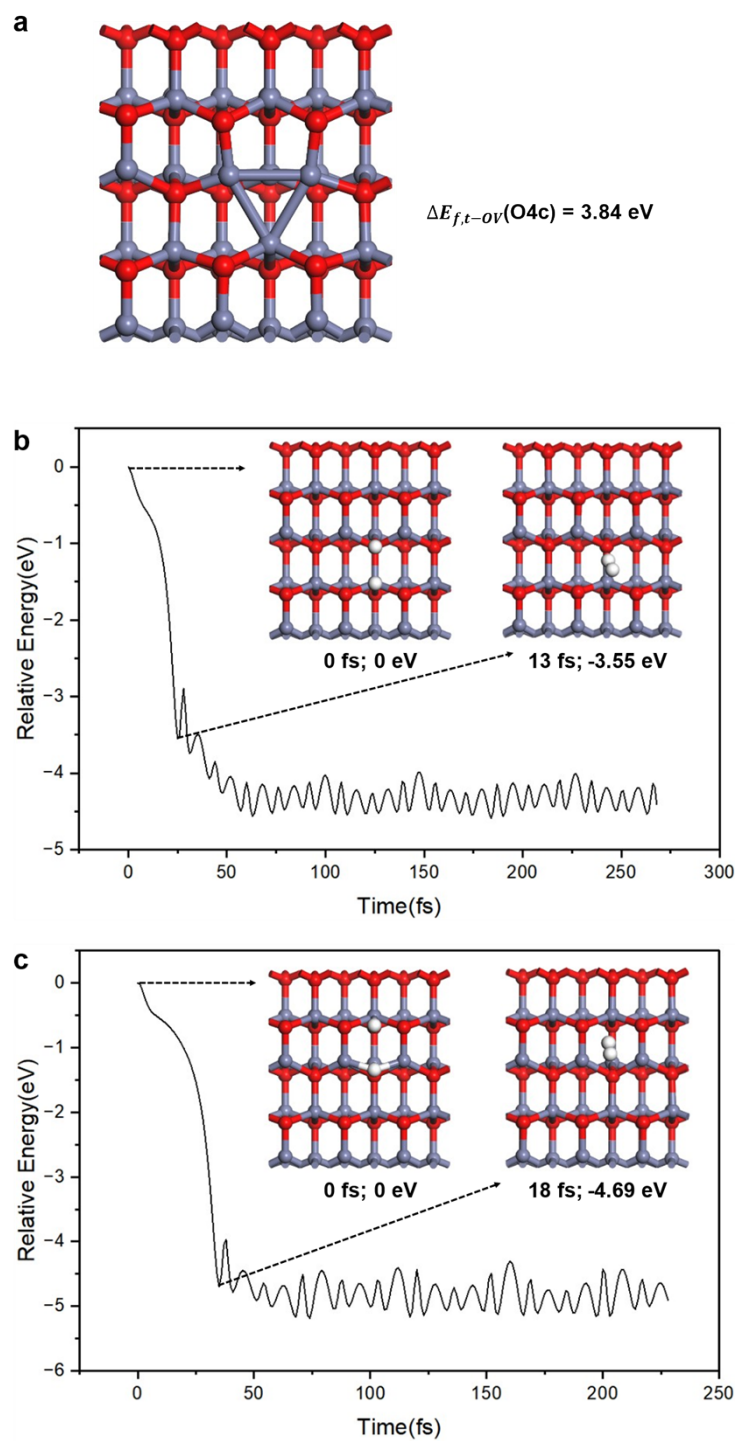


Figure S3. (a) Thermal induced OV generated by O_{4c} on the subsurface; (b) AIMD simulation of two H atoms adsorbed at Zn_{4c} - O_{4c} dimer; (b) AIMD simulation of two H atoms adsorbed at Zn_{4c} - O_{4c} trench.

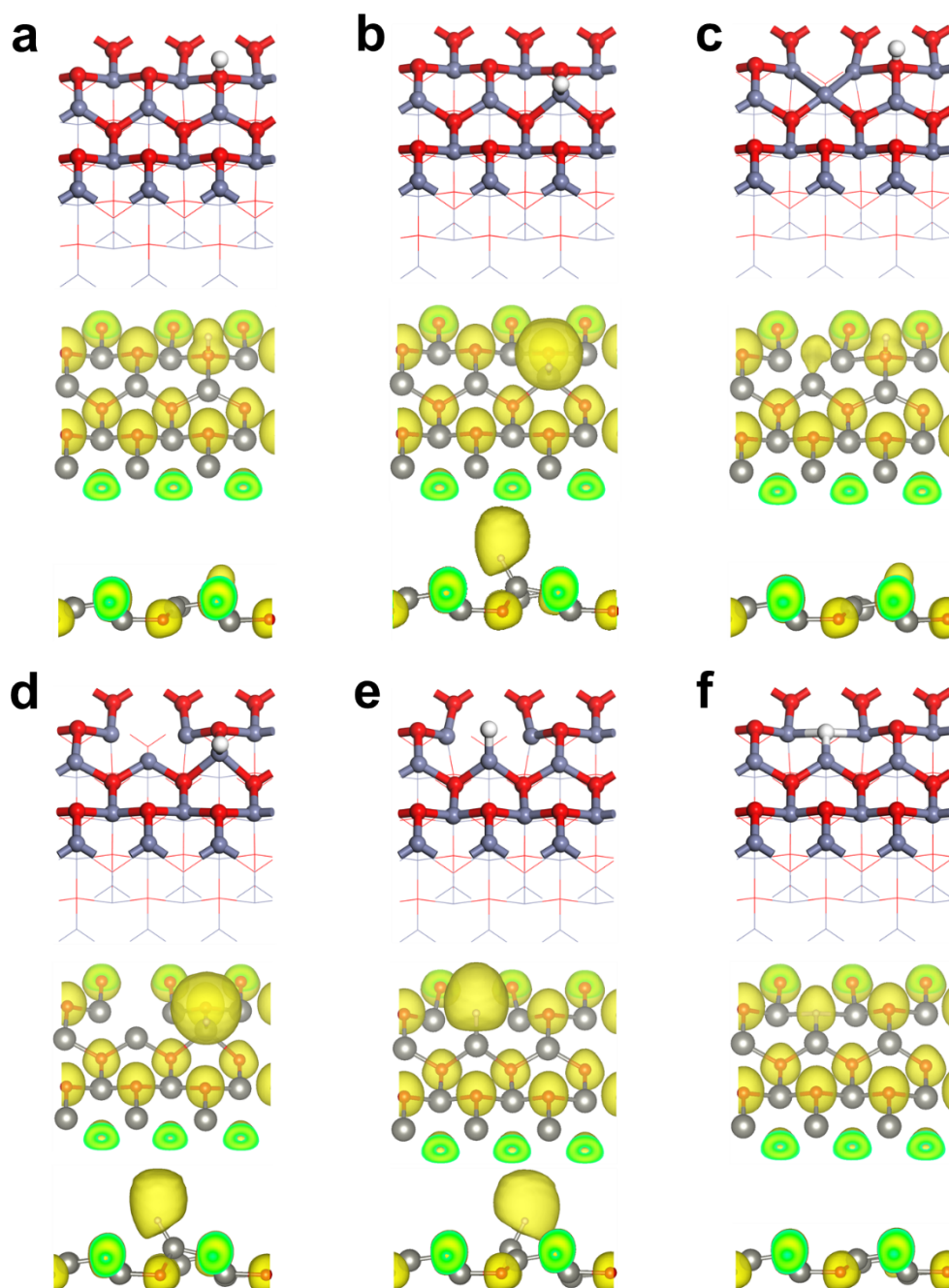


Figure S4. Structural models (top) and ELF analysis (middle and bottom) showing a single hydrogen atom adsorbed at different sites: (a) O_{3c} site on the pristine surface, (b) Zn_{3c} site on the pristine surface, (c) O_{3c} site on the defect surface, (d) Zn_{3c} site on the defect surface, (e) Zn_a atom on the defect surface, and (f) the oxygen vacancy (OV) site on the defect surface. Gray balls represent Zn atoms, red balls denote O atoms, and white spheres correspond to H atoms.

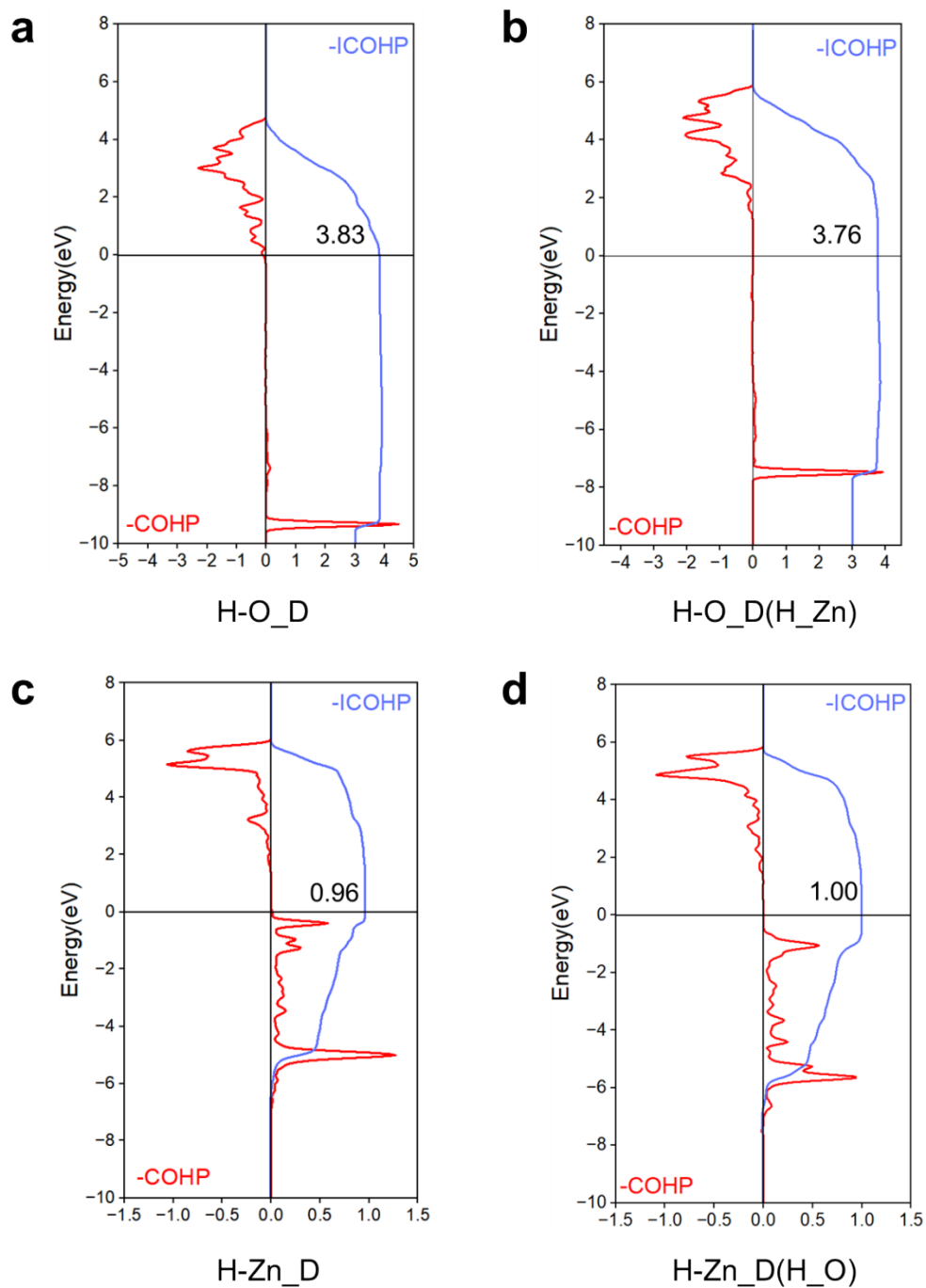


Figure S5. Crystal orbital Hamilton population (COHP) analyses of H–O and H–Zn bonds on defective ZnO ($10\bar{1}0$) surfaces under different pre-adsorption conditions. (a) H–O bond on a defect surface without pre-adsorbed H; (b) H–O bond on a defect surface with one H pre-adsorbed at the dimer-Zn site; (c) H–Zn bond on a defect surface without pre-adsorbed H; (d) H–Zn bond on a defect surface with one H pre-adsorbed at the dimer-O site. The numbers in the figure denote the $-ICOHP$ values at the Fermi level, and larger values indicate stronger bonds.

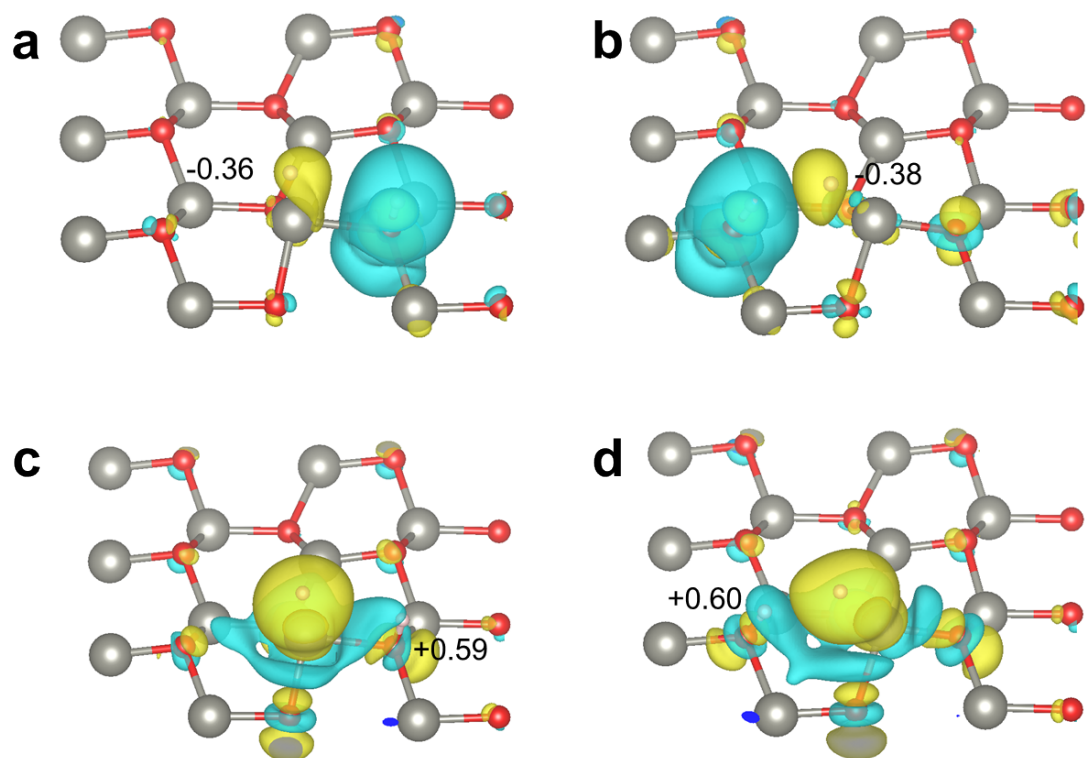


Figure S6. Charge-density difference plots for adsorption of a second H atom at different sites on the pristine ZnO ($10\bar{1}0$) surface with a pre-adsorbed H atom: (a) dimer-O, (b) trench-O, (c) dimer-Zn, and (d) trench-Zn. The numbers indicate the Bader charge of the pre-adsorbed H atom in the co-adsorbed configuration.

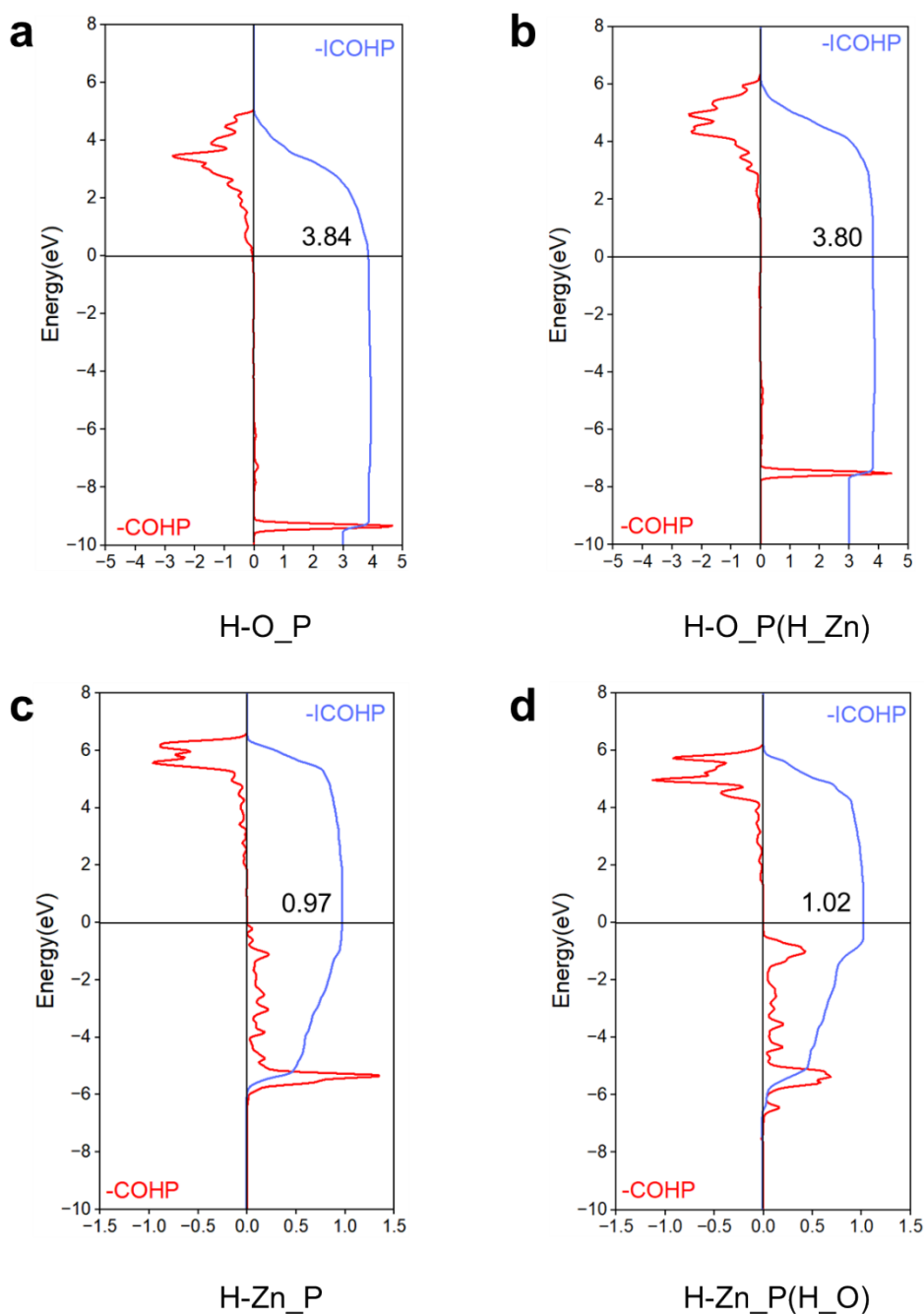


Figure S7. Crystal orbital Hamilton population (COHP) analyses of H-O and H-Zn bonds on pristine ZnO ($10\bar{1}0$) surfaces under different pre-adsorption conditions. (a) H-O bond on a pristine surface without pre-adsorbed H; (b) H-O bond on a pristine surface with one H pre-adsorbed at the dimer-Zn site; (c) H-Zn bond on a pristine surface without pre-adsorbed H; (d) H-Zn bond on a pristine surface with one H pre-adsorbed at the dimer-O site. The numbers in the figure denote the -ICOHP values at the Fermi level, and larger values indicate stronger bonds.

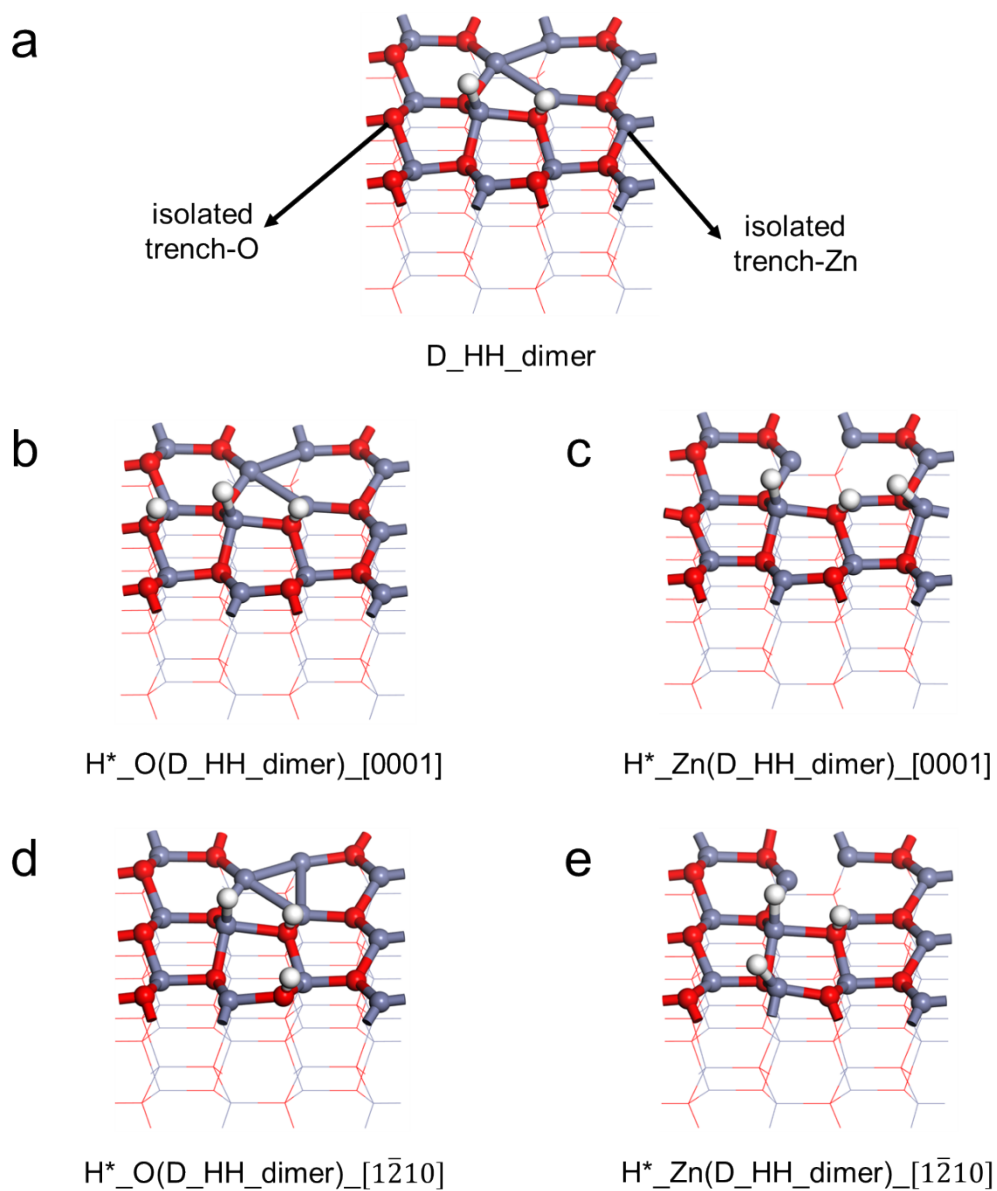


Figure S8. Structural models of various configurations on the defective ZnO ($10\bar{1}0$) surface. (a) A Zn–O dimer pre-adsorbed with two H atoms; (b–e) Configurations with an additional H atom adsorbed at different sites relative to the structure in (a): (b) adjacent O atom along the $[0001]$ direction, (c) adjacent Zn atom along the $[0001]$ direction, (d) adjacent O atom along the $[1\bar{2}10]$ direction, (e) adjacent Zn atom along the $[1\bar{2}10]$ direction.

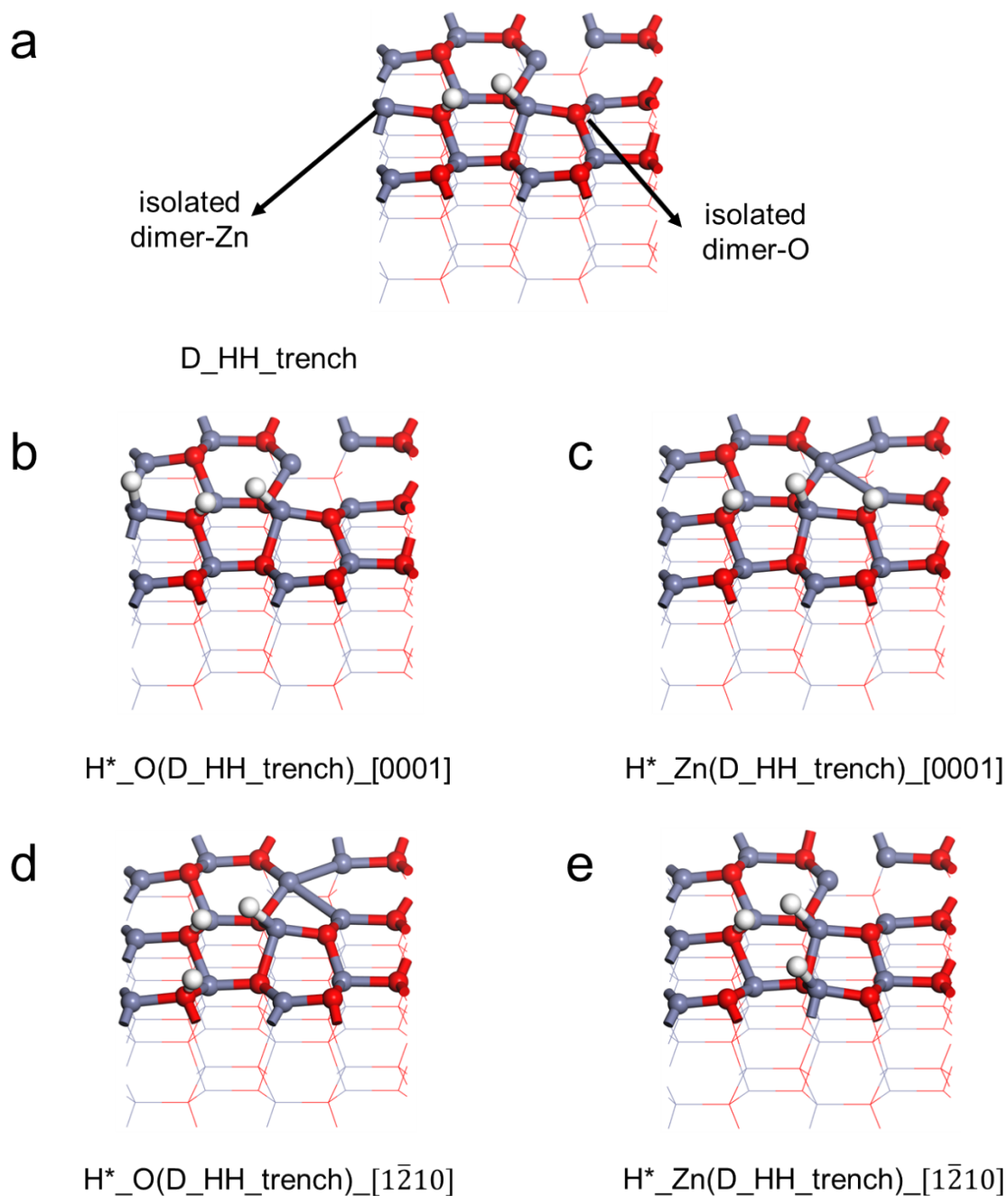


Figure S9. Structural models of various configurations on the defective ZnO ($10\bar{1}0$) surface. (a) A Zn–O trench pre-adsorbed with two H atoms; (b–e) Configurations with an additional H atom adsorbed at different sites relative to the structure in (a): (b) adjacent O atom along the $[0001]$ direction, (c) adjacent Zn atom along the $[0001]$ direction, (d) adjacent O atom along the $[1210]$ direction, (e) adjacent Zn atom along the $[1210]$ direction.

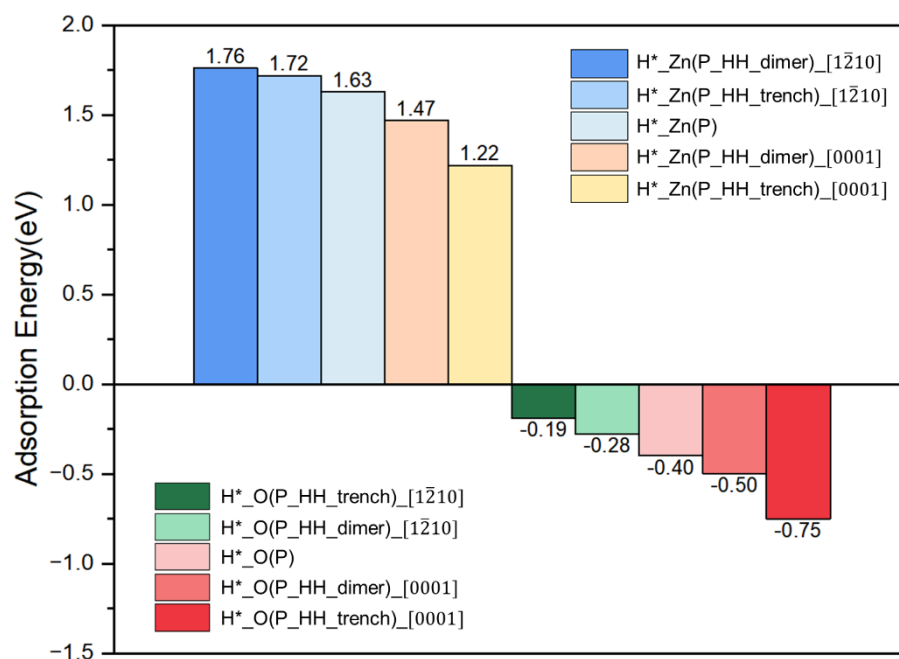


Figure S10. The adsorption energies of the next H atom on adjacent Zn or O atoms located along the $[1\bar{2}10]$ and $[0001]$ directions after pre-adsorbing one H_2 molecule at a Zn-O dimer or Zn-O trench compared to the values on the pristine $(10\bar{1}0)$ surface without any pre-adsorbed H.

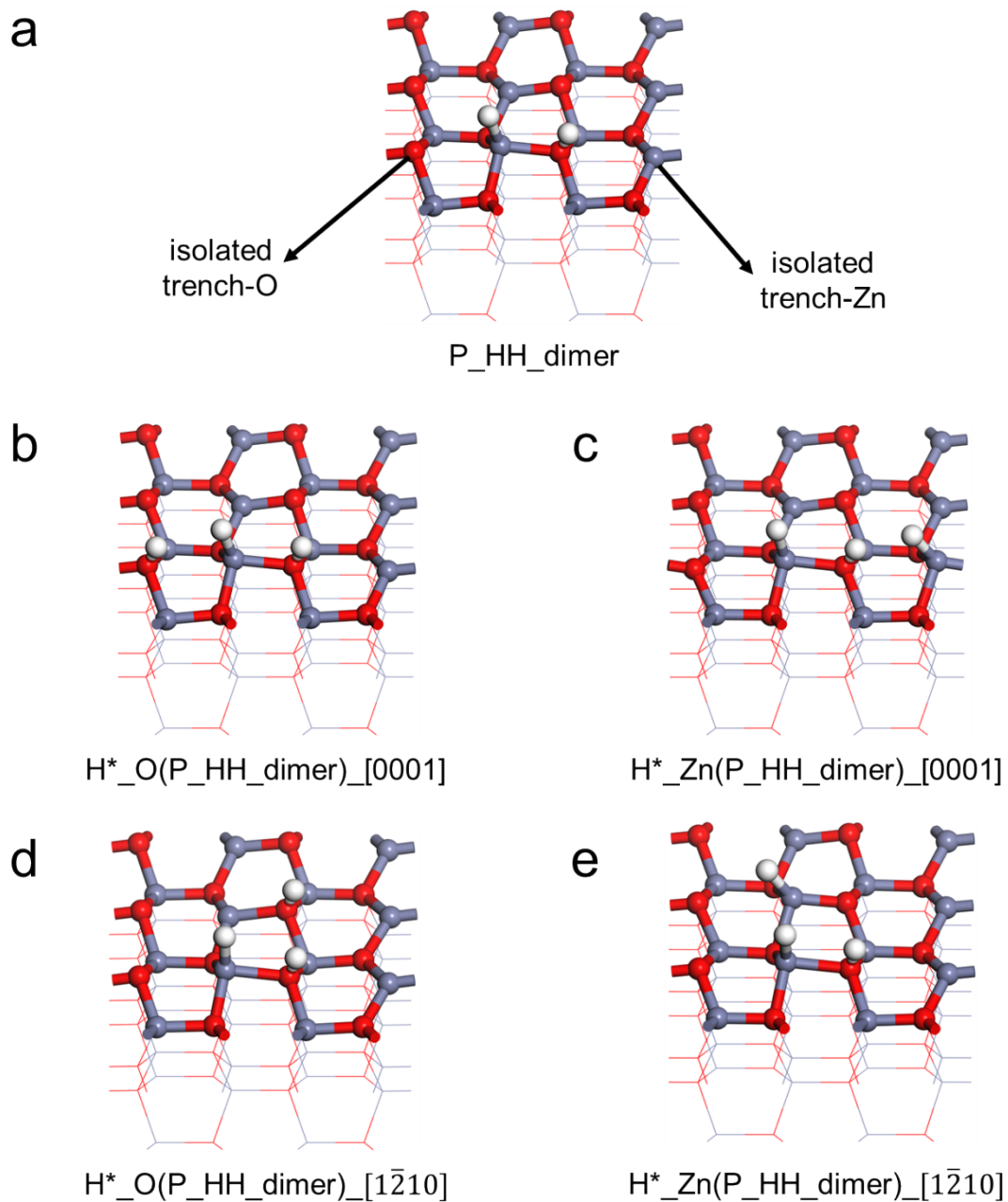


Figure S11. Structural models of various configurations on the pristine ZnO ($10\bar{1}0$) surface. (a) A Zn–O dimer pre-adsorbed with two H atoms; (b–e) Configurations with an additional H atom adsorbed at different sites relative to the structure in (a): (b) adjacent O atom along the $[0001]$ direction, (c) adjacent Zn atom along the $[0001]$ direction, (d) adjacent O atom along the $[1210]$ direction, (e) adjacent Zn atom along the $[1210]$ direction.

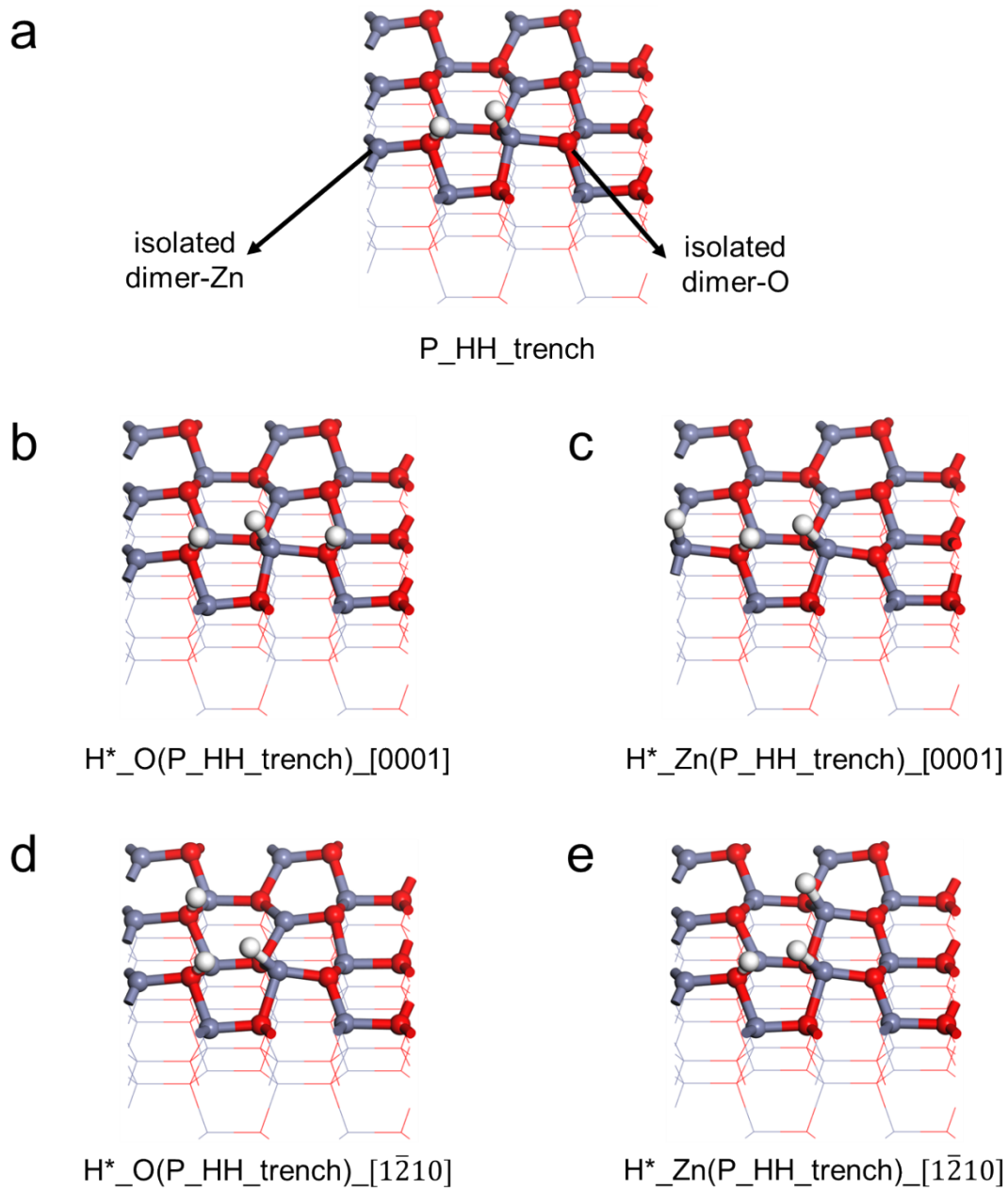


Figure S12. Structural models of various configurations on the pristine ZnO ($10\bar{1}0$) surface. (a) A Zn–O trench pre-adsorbed with two H atoms; (b–e) Configurations with an additional H atom adsorbed at different sites relative to the structure in (a): (b) adjacent O atom along the $[0001]$ direction, (c) adjacent Zn atom along the $[0001]$ direction, (d) adjacent O atom along the $[1210]$ direction, (e) adjacent Zn atom along the $[1210]$ direction.

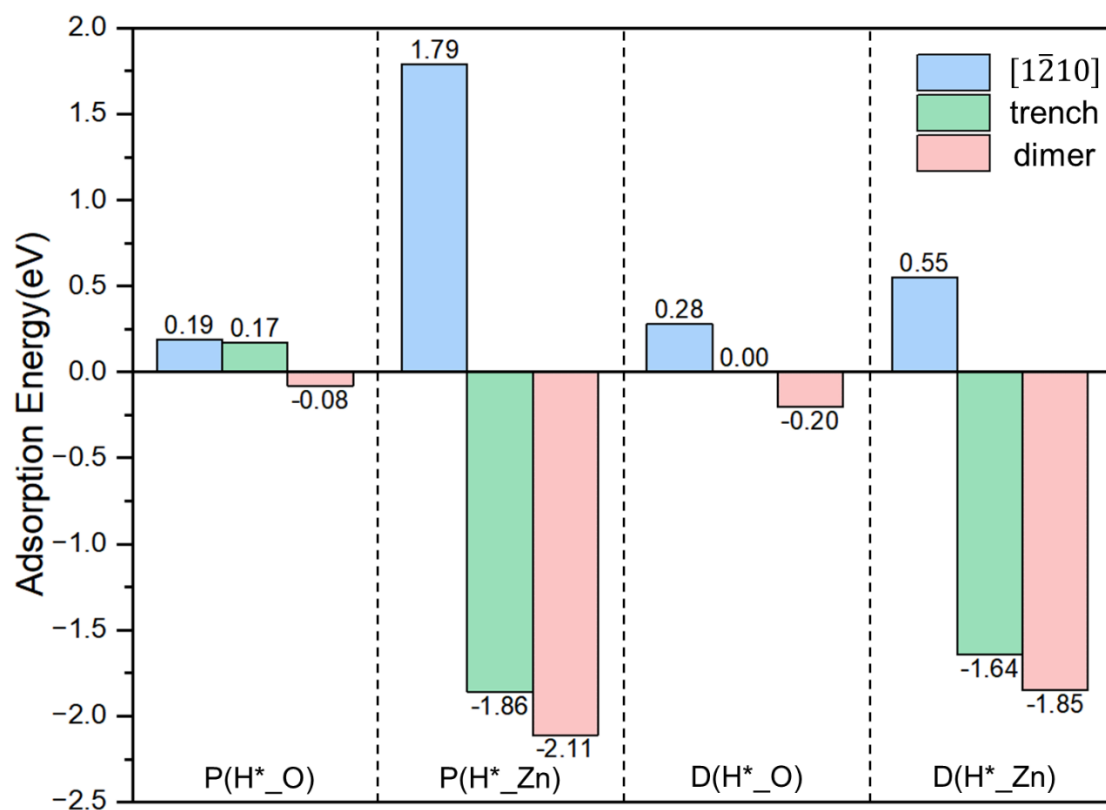


Figure S13. Adsorption energies of a second H atom on surfaces with different pre-adsorption conditions. From left to right, the four panels correspond to: a pristine surface with one H atom pre-adsorbed on an O atom, a pristine surface with one H atom pre-adsorbed on a Zn atom, a defective surface with one H atom pre-adsorbed on an O atom, and a defective surface with one H atom pre-adsorbed on a Zn atom. Different colors indicate the relative position of the second H atom: blue for adsorption along the $[1\bar{2}10]$ direction, green for adsorption at trench-O or trench-Zn sites, and pink for adsorption at dimer-O or dimer-Zn sites.

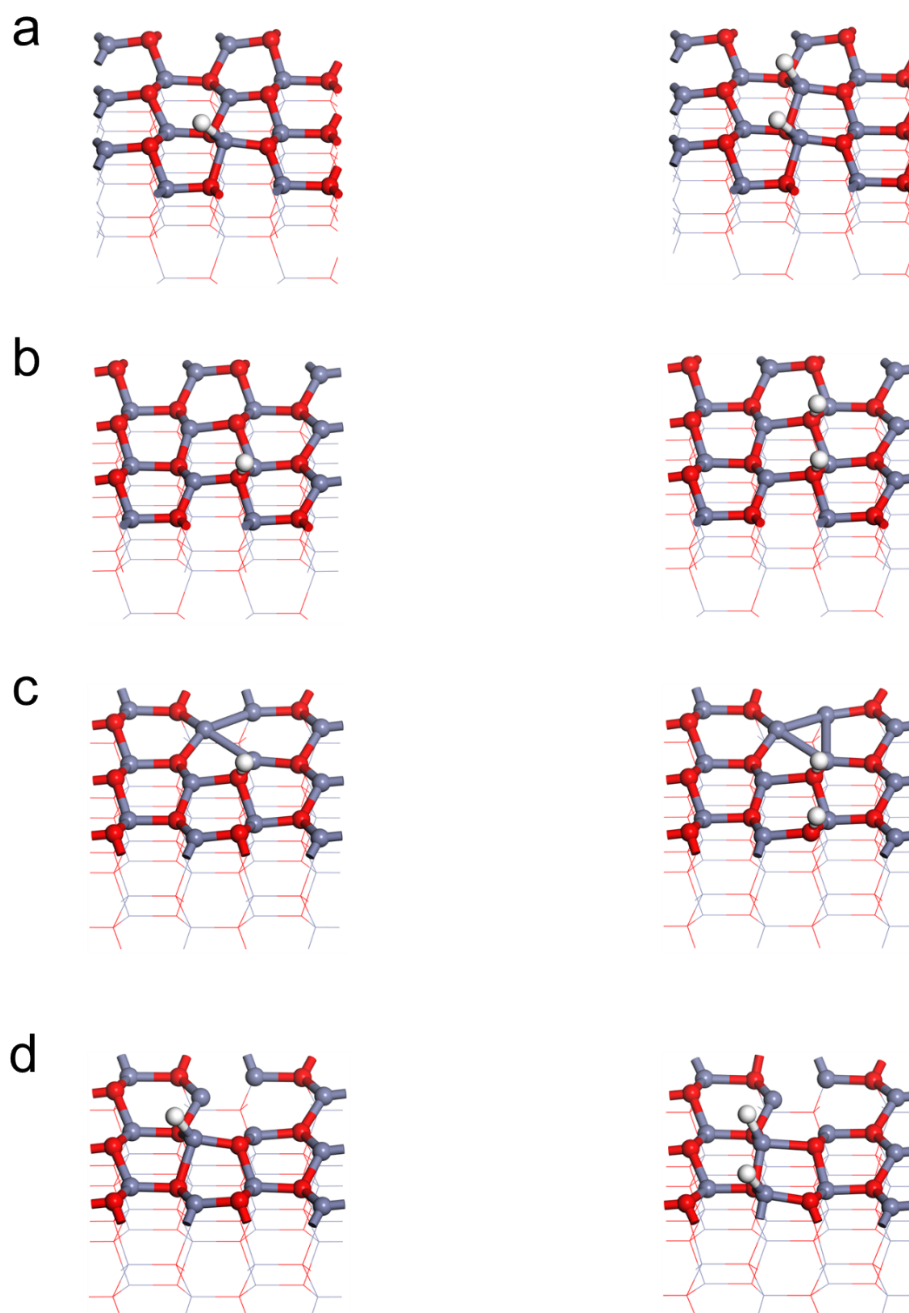


Figure S14. Schematic configurations of an additional H atom adsorbed on the neighboring site along the $[12\bar{1}0]$ direction on ZnO $(10\bar{1}0)$ surfaces that are pre-covered by a single hydrogen atom: (a) the pre-adsorbed H atom is bound to a three-coordinated Zn atom on the pristine surface; (b) the pre-adsorbed H atom is bound to a three-coordinated O atom on the pristine surface; (c) the pre-adsorbed H atom is bound to a three-coordinated O atom adjacent to an oxygen vacancy (defective surface); (d) the pre-adsorbed H atom is bound to a two-coordinated Zn atom next to an oxygen vacancy (defective surface).

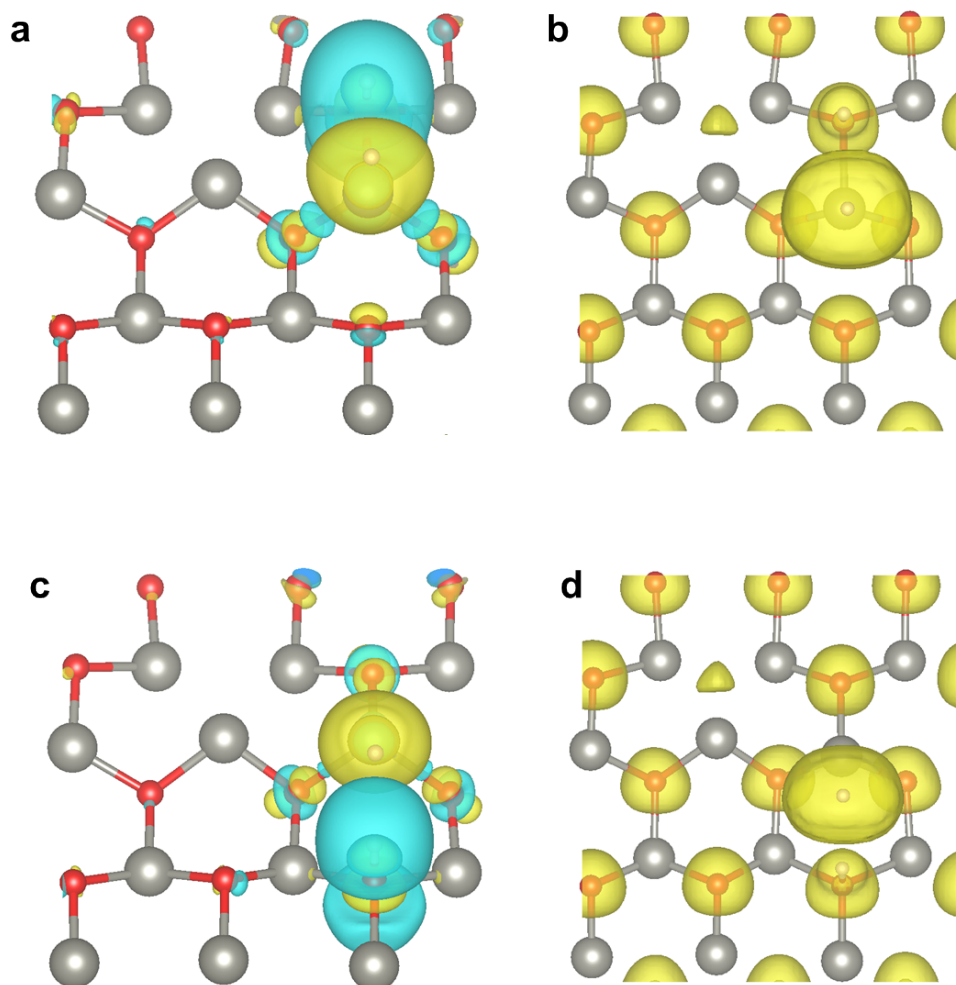


Figure S15. (a, c) Charge-density difference maps before and after H₂ chemisorption at (a) Zn–O dimer and (c) Zn–O trench sites. Yellow regions indicate electron accumulation, while blue regions represent electron depletion. (b, d) Electron localization function (ELF) maps for H₂ chemisorbed at the Zn–O dimer and Zn–O trench sites, respectively. Yellow isosurfaces represent regions of electron localization.

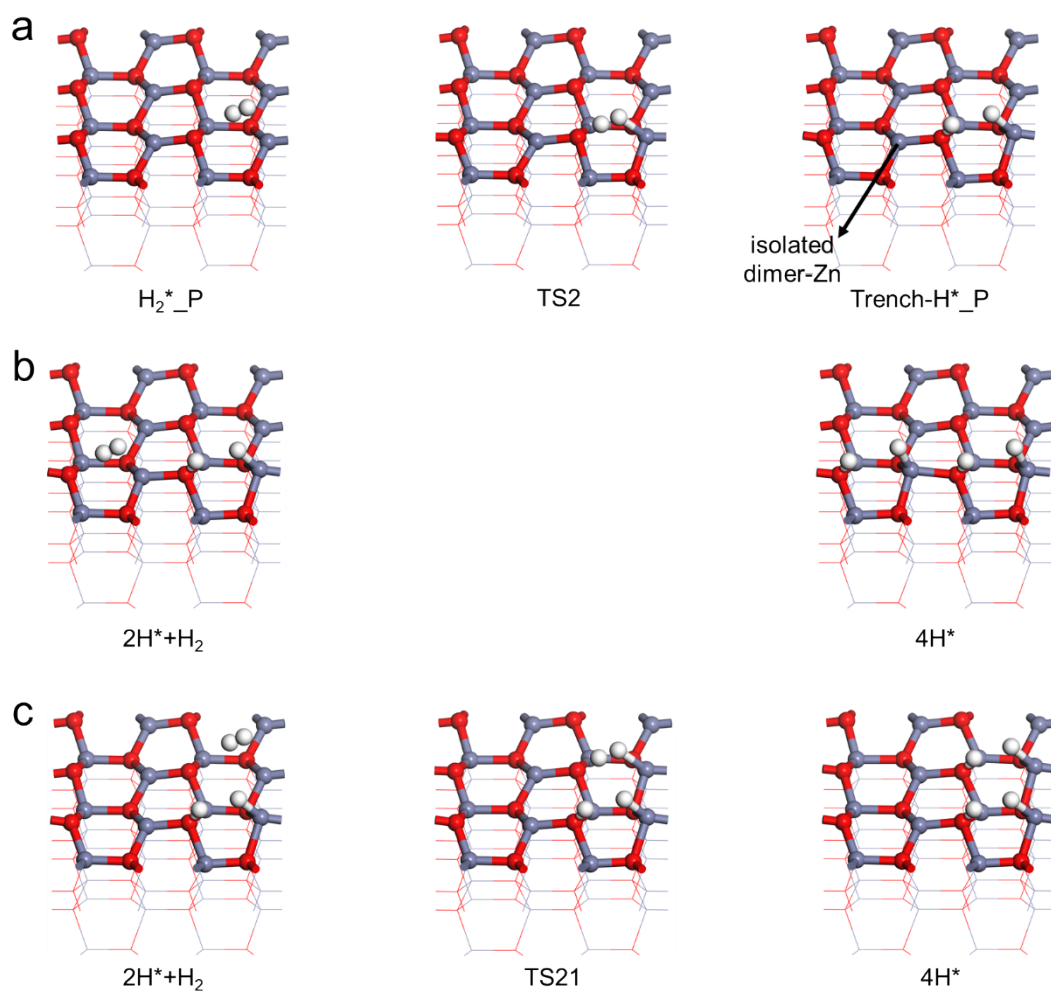


Figure S16. Configurations for sequential H_2 dissociation on the pristine ZnO ($10\bar{1}0$) surface. (a) The first H_2 molecule dissociates on a Zn–O trench site. (b) The second H_2 molecule dissociates on the neighboring Zn–O pair located in the $[0001]$ direction from the first dissociation site. (c) The second H_2 molecule dissociates on the adjacent Zn–O pair located in the $[12\bar{1}0]$ direction from the first dissociation site.

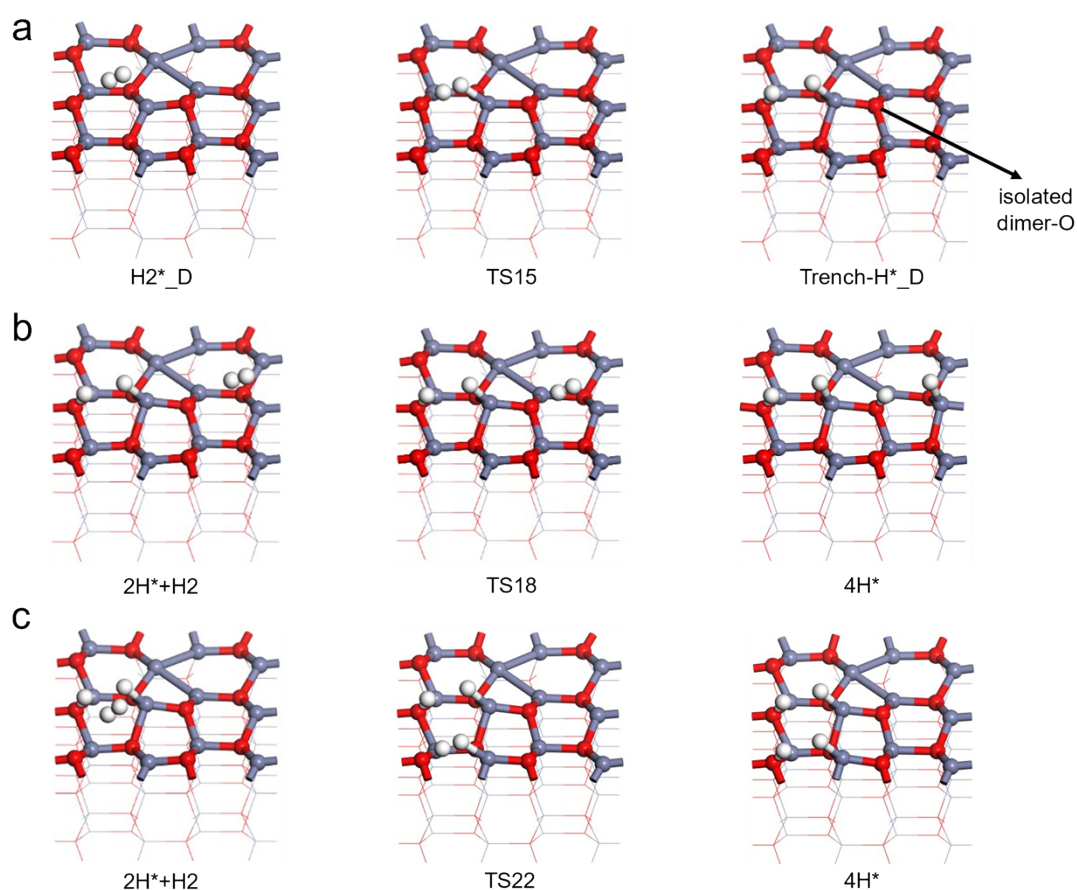


Figure S17. Configurations for sequential H_2 dissociation on the defect ZnO ($10\bar{1}0$) surface. (a) The first H_2 molecule dissociates on a Zn–O trench site. (b) The second H_2 molecule dissociates on the neighboring Zn–O pair located in the $[0001]$ direction from the first dissociation site. (c) The second H_2 molecule dissociates on the adjacent Zn–O pair located in the $[12\bar{1}0]$ direction from the first dissociation site.

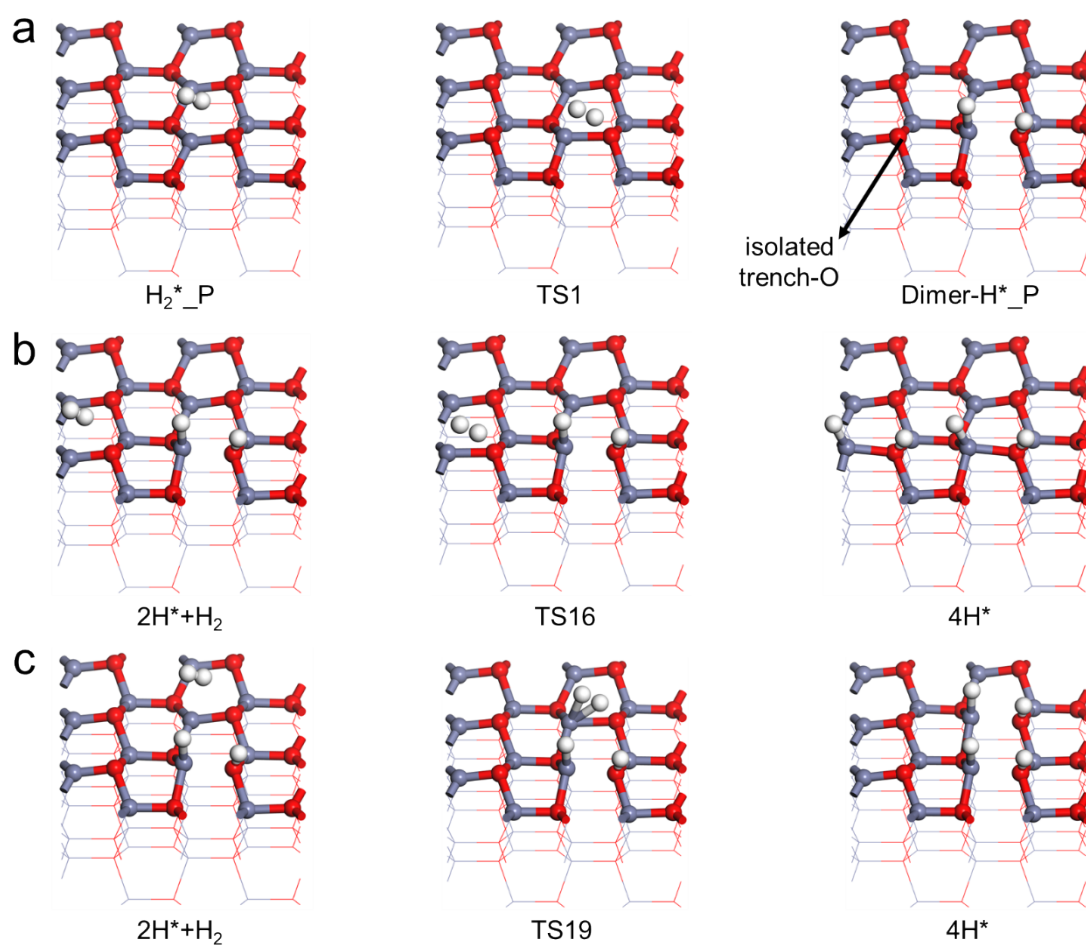


Figure S18. Configurations for sequential H_2 dissociation on the pristine ZnO ($10\bar{1}0$) surface. (a) The first H_2 molecule dissociates on a Zn–O dimer site. (b) The second H_2 molecule dissociates on the neighboring Zn–O pair located in the $[0001]$ direction from the first dissociation site. (c) The second H_2 molecule dissociates on the adjacent Zn–O pair located in the $[1\bar{2}10]$ direction from the first dissociation site.

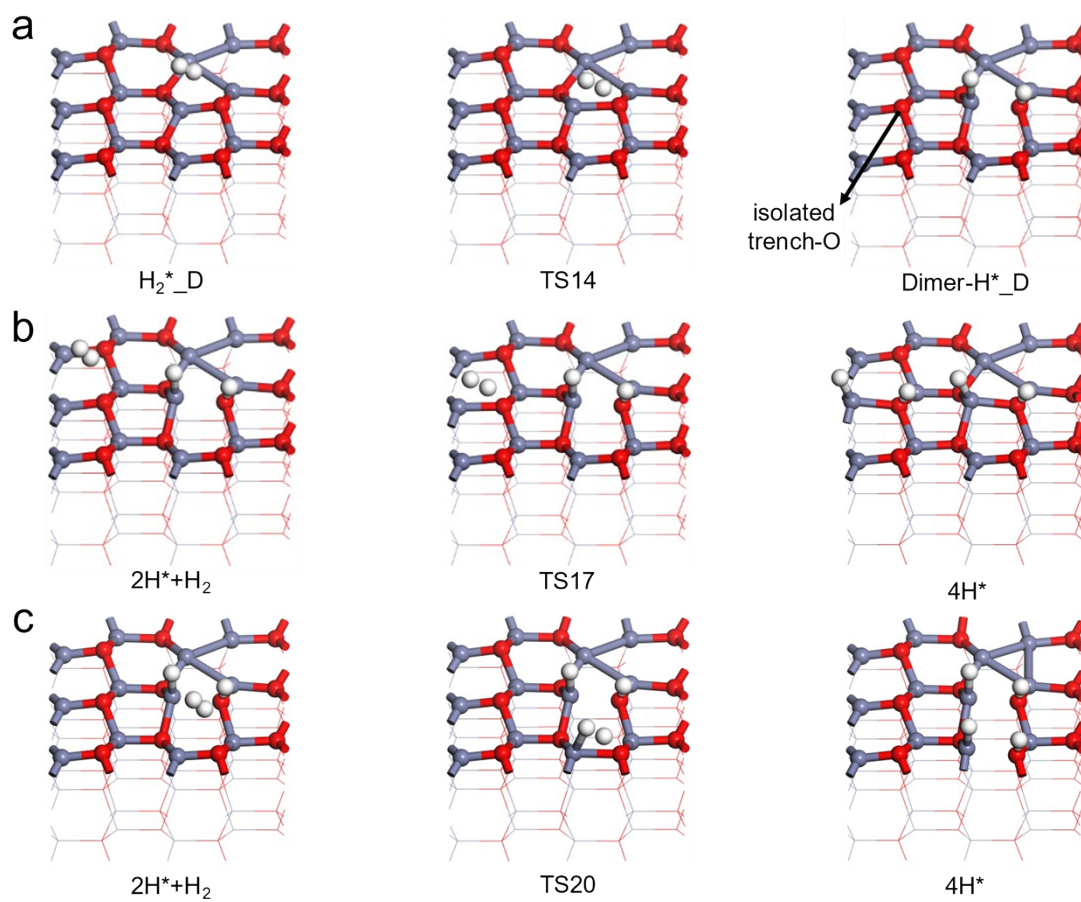


Figure S19. Configurations for sequential H_2 dissociation on the defect ZnO ($10\bar{1}0$) surface. (a) The first H_2 molecule dissociates on a Zn–O dimer site. (b) The second H_2 molecule dissociates on the neighboring Zn–O pair located in the $[0001]$ direction from the first dissociation site. (c) The second H_2 molecule dissociates on the adjacent Zn–O pair located in the $[12\bar{1}0]$ direction from the first dissociation site.

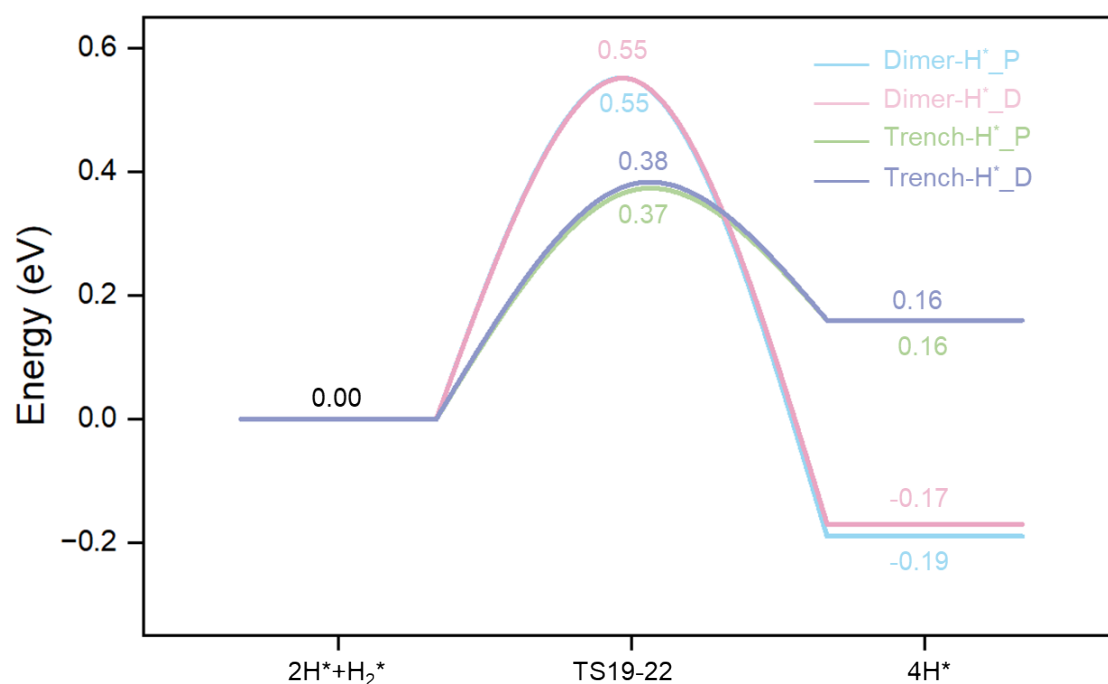


Figure S20. Potential-energy surfaces for the adsorption of a second H₂ molecule along the [1210] direction on ZnO (10 $\bar{1}$ 0) surfaces that are pre-covered by one H₂. Blue curve: pristine surface in which the first H₂ dissociatively adsorbs on a Zn–O dimer; pink curve: defect surface in which the first H₂ dissociatively adsorbs on the same Zn–O dimer; green curve: pristine surface in which the first H₂ dissociatively adsorbs on a Zn–O trench; purple curve: defect surface in which the first H₂ dissociatively adsorbs on the Zn–O trench.

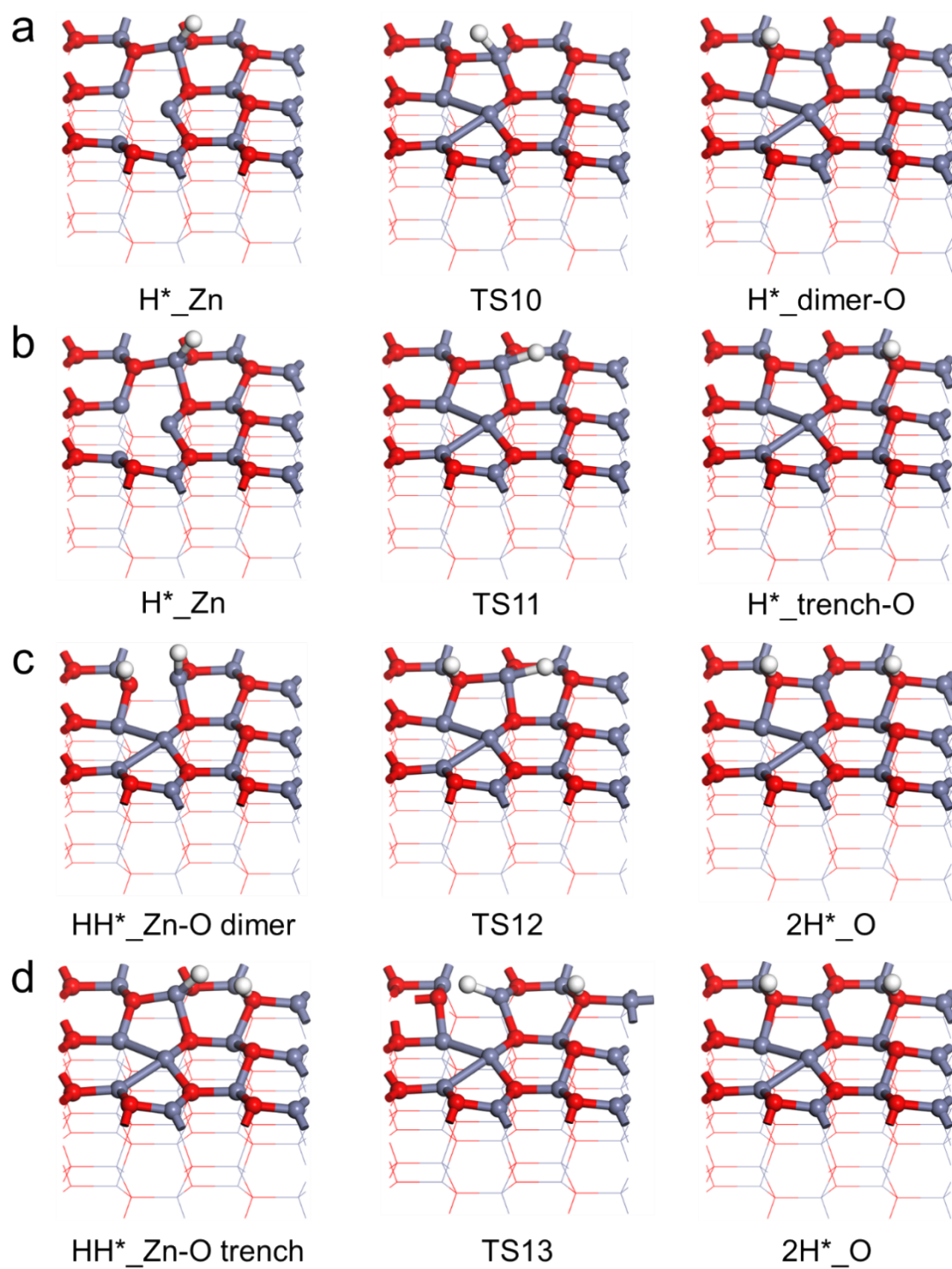


Figure S21. Schematic structures of the key intermediates and transition states for hydrogen migration from a Zn site to an O site under four distinct scenarios. Panels (a-d) correspond to the green, purple, blue, and pink pathways plotted in Figure S28, respectively.

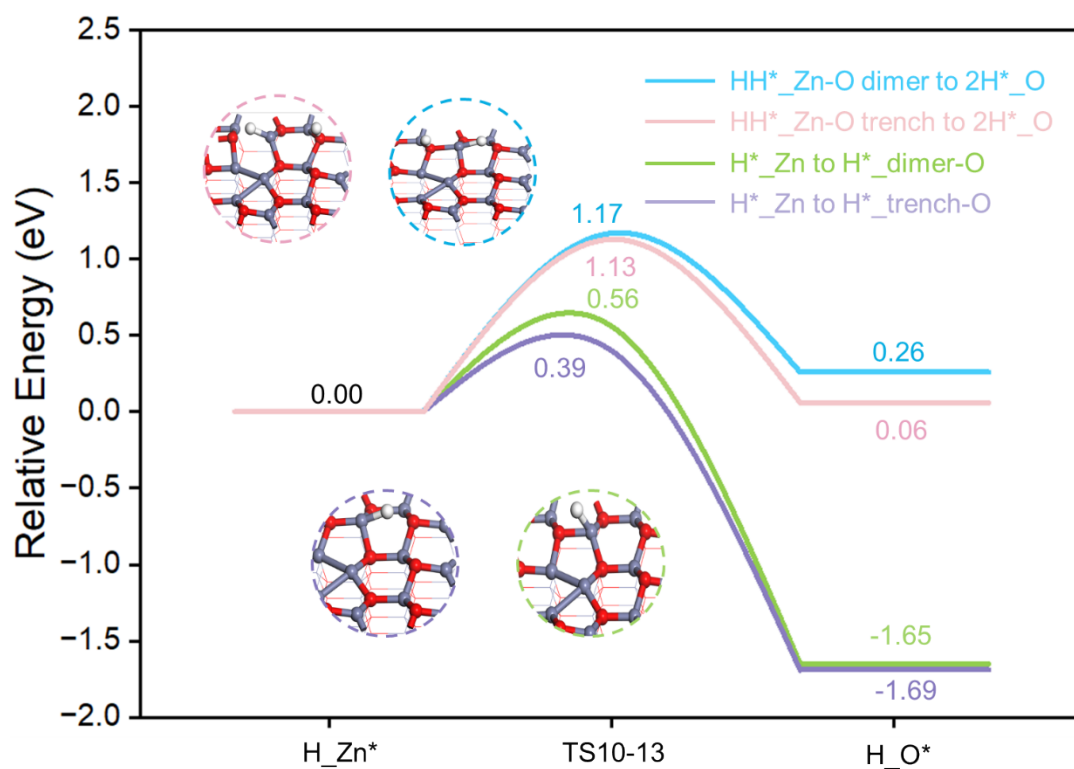


Figure S22. Potential energy surfaces for the diffusion of a hydrogen atom from a Zn_{3c} site to an O_{3c} site on ZnO ($10\bar{1}0$). Blue curve: a Zn–O dimer bearing two pre-adsorbed H atoms, with one H migrating from Zn to O; pink curve: a Zn–O trench bearing two pre-adsorbed H atoms, with one H migrating from Zn to O; green curve: a single H atom on a Zn site migrating to a dimer O site; purple curve: a single H atom on a Zn site migrating to a trench-O site.

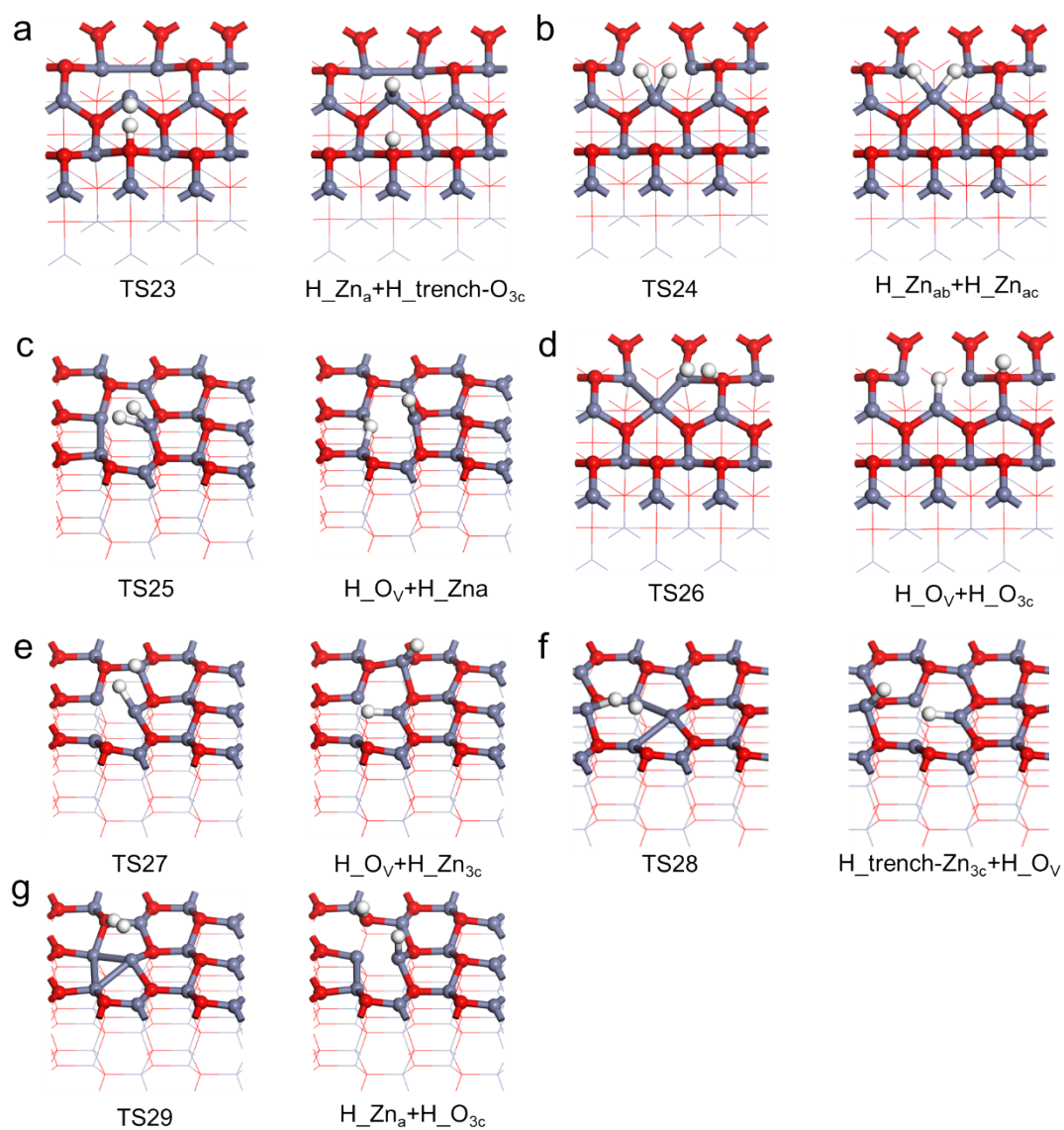


Figure S23. Transition-state structures and final adsorption configurations for seven H₂ dissociation pathways associated with the OV-Zn₃ site.

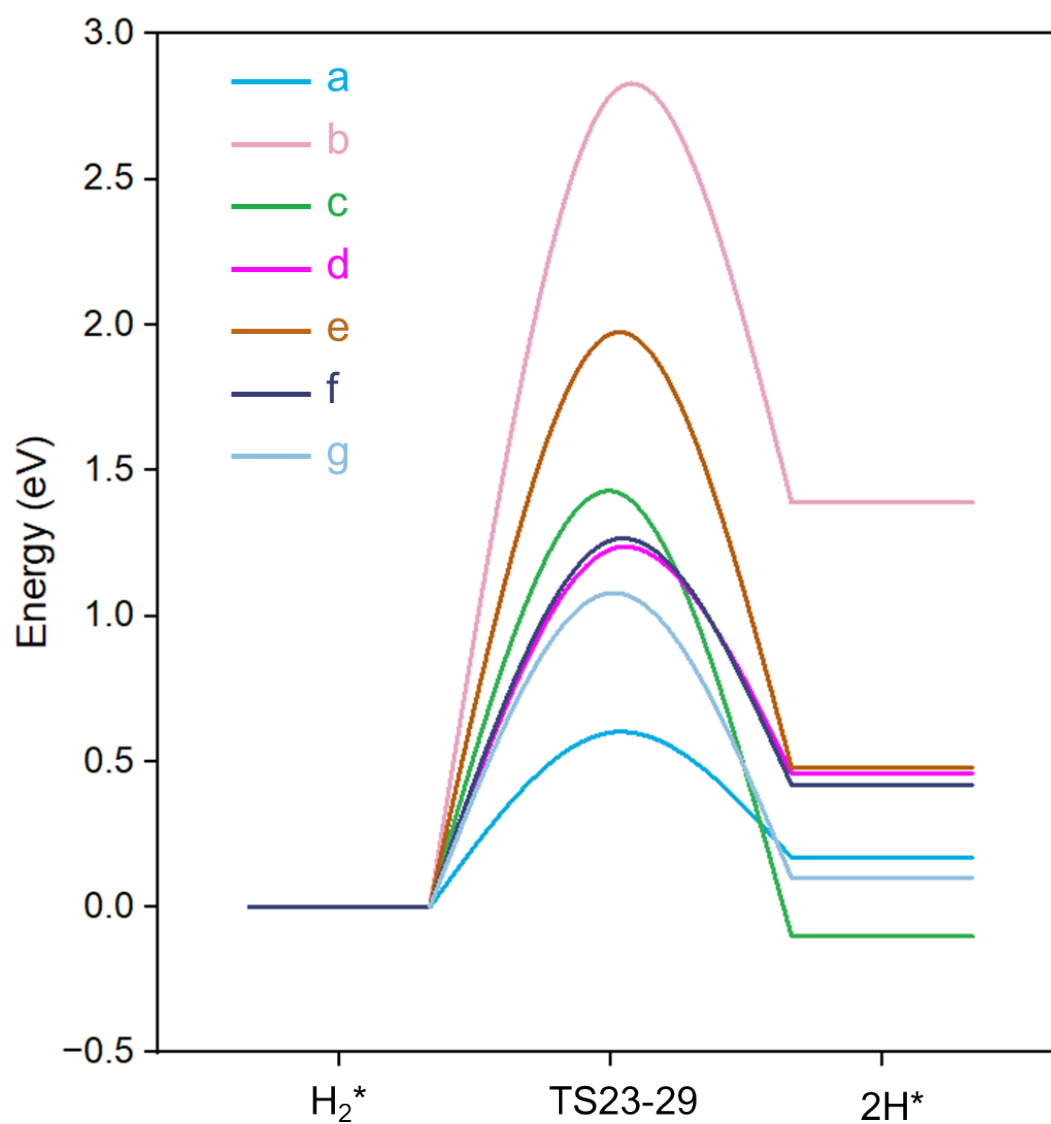


Figure S24. Potential energy surfaces for seven H₂ dissociation pathways associated with the OV-Zn₃ complex. Energy values are summarized in **Table S1**, and corresponding structural information is provided in **Figure S23**.

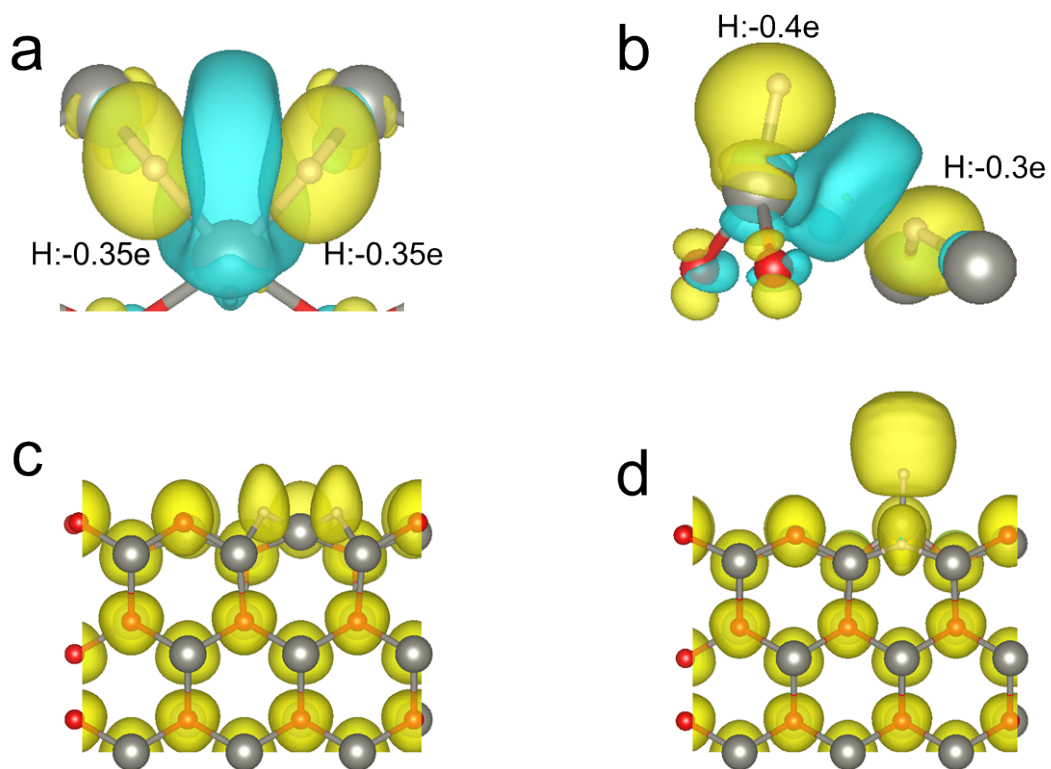


Figure S25. (a, c) Charge-density difference maps and electron localization function (ELF) maps for H_2 homolytic dissociation across the $\text{Zn}_a\text{-Zn}_b$ and $\text{Zn}_a\text{-Zn}_c$ bridge sites, respectively. (b, d) Charge-density difference maps and ELF maps for H_2 homolytic dissociation across the OV and Zn_a sites.

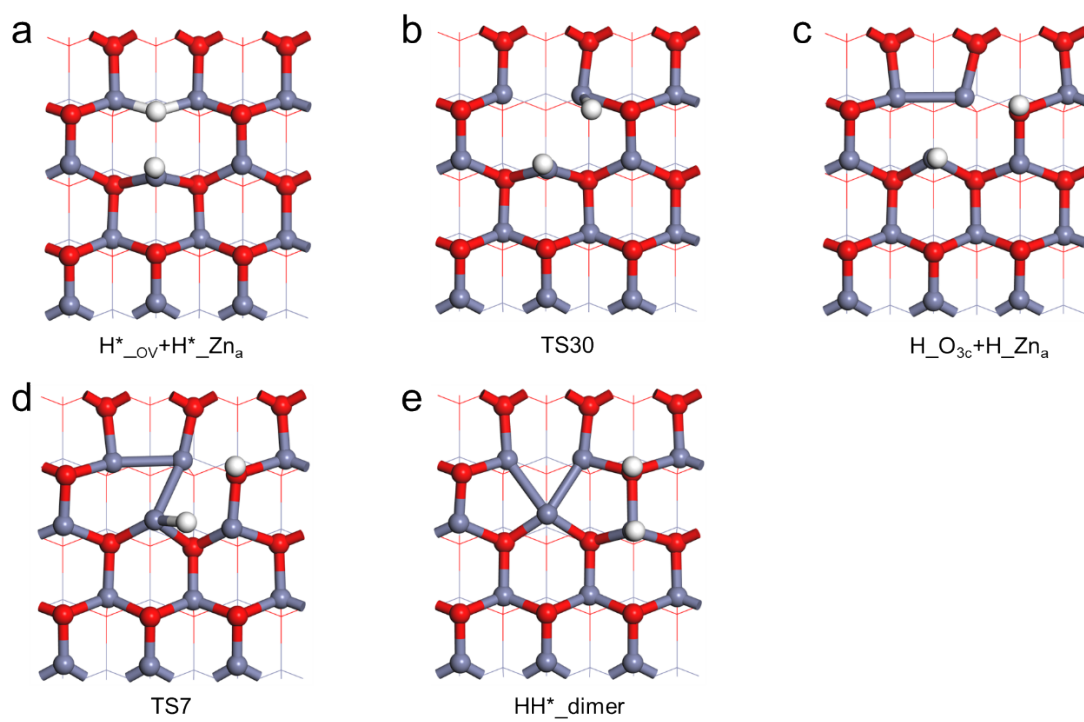


Figure S26. Structural representations of key intermediates along the H_2 diffusion pathwayII.

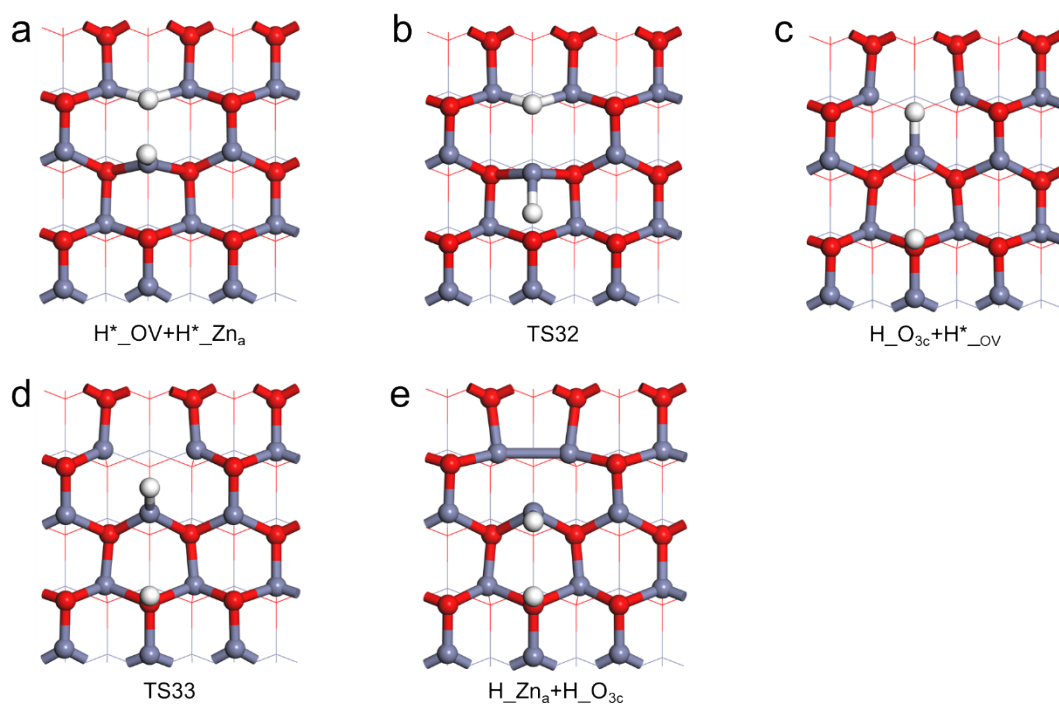


Figure S27. Schematic representations of key adsorption configurations during the diffusion process of two H atoms co-adsorbed at the OV and Zn_a sites along the $[0001]$ direction.

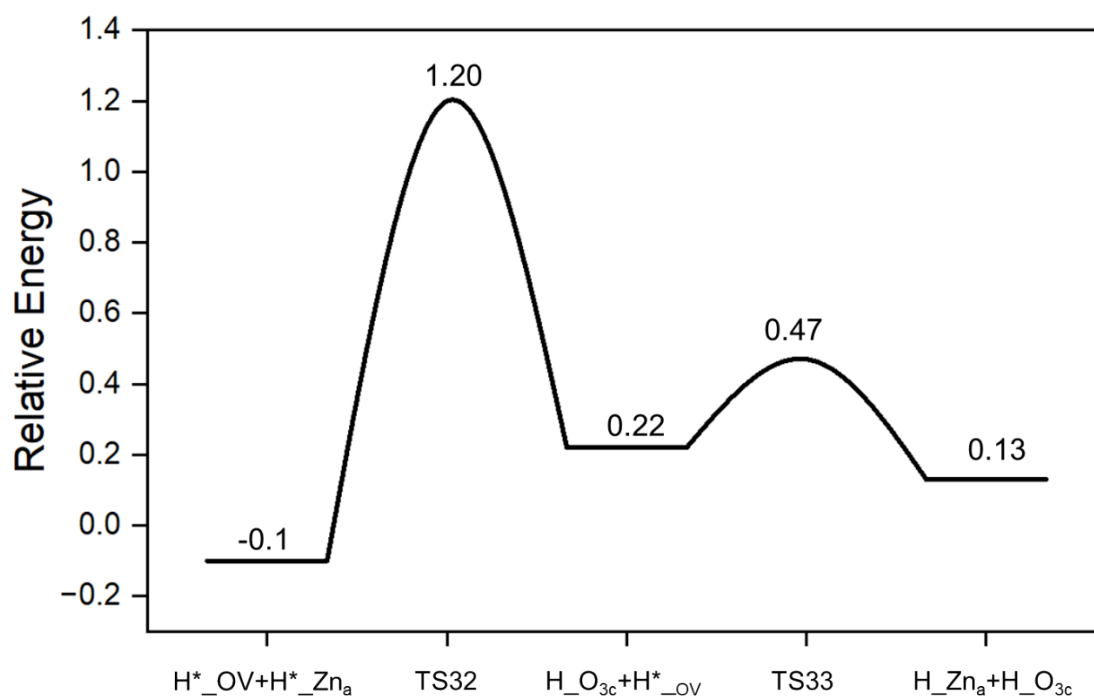


Figure S28. Potential energy surface for the diffusion of two H atoms co-adsorbed at the OV and Zn_a sites along the [0001] direction. Relative energies are referenced to the state in which an H₂ molecule is physisorbed on the defective surface.

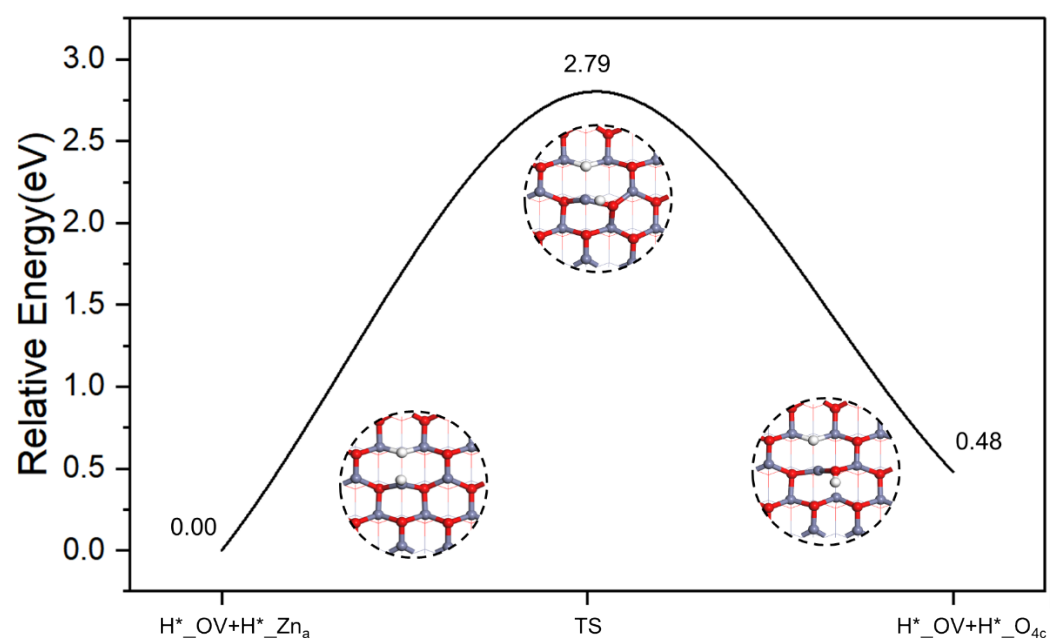


Figure S29. Potential energy surface for the migration of an H atom at Zn_a to a O_{4c} atom.

Table S1. Energetic information for seven H₂ dissociation pathways associated with the OV–Zn₃ ensemble. IS denotes the initial states, TS the transition states, and FS the final states.

PAT	Relative energy of IS	Relative energy of TS	Relative energy of FS
H	(eV)	(eV)	(eV)
a	0	0.60	0.17
b	0	2.79	1.39
c	0	1.43	-0.10
d	0	1.23	0.46
e	0	1.97	0.48
f	0	1.26	0.42
g	0	1.08	0.10

Table S2. Contribution of the OV–Zn₃ complex to the chemisorption of H₂ at the indicated surface sites. The contribution is expressed as the ratio of the electrons gained or lost by the complex to the net charge gained or lost by the adsorbate. Bader charges are reported in units of e; positive values denote electron loss and negative values denote electron gain.

	Charge of Zna	Charge of Znb	Charge of Znc	Charge of O _{OV}	Total charge of OV– Zn ₃ (O _{OV} +Zn ₃)	H adsorption–induced charge loss of Zn ₃ (O _{OV} +Zn ₃)	Total charge of H	Contribution of OV–Zn ₃ (O _{OV} +Zn ₃)
P	+1.16	+1.21	+1.21	-1.16	+2.42	/	/	/
D	+0.62	+0.94	+0.94	/	+2.5	/	/	/
a	+0.75	+0.78	+0.81	/	+2.34	-0.16	-0.27	-59.26%
b	+1.03	+1.08	+1.08	/	+3.19	+0.69	-0.70	98.57%
c	+0.92	+1.11	+1.11	/	+3.14	+0.64	-0.70	91.43%
d	+1.02	+1.11	+1.11	/	+3.04	+0.54	-0.17	317.65%
e	+1.06	+1.13	+1.15	/	+3.34	+0.84	-0.73	115.07%
f	+1.03	+1.14	+1.14	/	+3.31	+0.81	-0.73	110.96%
g	+0.81	+0.83	+0.71	/	+2.35	-0.15	-0.23	-65.22%